

# Search for Exotic Hybrids in the Coherent Production off $^4\text{He}$

G. Asryan, I. Aznauryan<sup>1</sup>, K. Egiyan  
Yerevan Physics Institute, Yerevan, Armenia

G. Dodge, S. Kuhn, S. Stepanyan<sup>1,2,3</sup>, L. Weinstein  
Old Dominion University, Norfolk, VA, USA

A. Afanasev, V. Burkert, H. Egiyan, L. Elouadrhiri, A. Freyberger, M. Mestayer,  
M. Nozar, E. Smith, D. Weygand  
Jefferson Lab, Newport News, VA, USA

C. Salgado, M. Khandaker  
Norfolk State University, Norfolk, VA, USA

P. Eugenio, A. Ostrovidov  
Florida State University, Tallahassee, FL, USA

V. Kubarovsky  
Rensselaer Polytechnic Institute, Troy, NY, USA  
and Jefferson Lab, Newport News, VA, USA

H. Funsten  
College of William and Mary, Williamsburg, VA, USA

G.P. Gilfoyle  
University of Richmond, Richmond, VA, USA

## Abstract

This experiment will search for  $J^{PC} = 1^{-+}$  exotic hybrids in the  $\pi\eta$  and  $\pi\eta'$  decay modes, using quasi-real photoproduction on  $^4\text{He}$ . Coherent production of  $t$ -channel mesons off the spin- and isospin-zero target will simplify significantly the PWA. The experiment will use a 6 GeV electron beam and the CLAS detector to search for exotic states in the mass range up to 2 GeV.

---

<sup>1</sup>Spokesperson

<sup>2</sup>Contact-person

<sup>3</sup>Also Jefferson Lab, Newport News, VA, USA

# Contents

<b>1</b>	<b>Introduction</b>	<b>3</b>
<b>2</b>	<b>Current status of <math>J^{PC} = 1^{-+}</math> hybrid</b>	<b>4</b>
2.1	Predictions for hybrids . . . . .	4
2.2	Experimental situation . . . . .	4
<b>3</b>	<b>Proposed Experiment</b>	<b>5</b>
<b>4</b>	<b>PWA Formalism.</b>	<b>8</b>
<b>5</b>	<b>Experimental Issues</b>	<b>10</b>
5.1	Proposed configuration. . . . .	11
5.2	CLAS performance. . . . .	12
<b>6</b>	<b>Cross Section and Expected Event Rate.</b>	<b>14</b>
6.1	Cross section formalism. . . . .	15
6.2	Event rate. . . . .	18
<b>7</b>	<b>Other Possible Channels</b>	<b>20</b>
7.1	Search for exotic meson in the $\phi\pi$ final state. . . . .	20
<b>8</b>	<b>Summary</b>	<b>21</b>

# 1 Introduction

The gluon, the gauge boson of QCD, carries a color charge. It can have a component characterizing it as a force and a component characterizing it as a constituent particle[1]. It can thus act as a particle and create a binding force to quarks arising from additional gluons interconnecting to the quarks. One thus expects a class of hadrons, hybrid mesons, comprised of a valence gluon bound to two quarks,  $gq\bar{q}$ . (In addition, there are expectations for the existence of a glueball meson consisting of a gluon loop,  $gg$ , and for existence of hybrid baryons  $gqqq$ ). Although evidence for gluons has been found in jet measurements and in deep inelastic scattering, an unambiguous signal of constituent glue has not been observed. The discovery of hybrids would be a strong confirmation of QCD, and important for understanding the non-perturbative structure of hadrons.

QCD models have made a variety of predictions for the masses, widths, and decay modes of hybrid  $gq\bar{q}$  states [1, 2, 3, 4, 5, 6]. The predicted mass of the lowest lying hybrid is  $\leq 2$  GeV. The best way, perhaps the only way, to search for hybrid states in this mass region is to look for states with exotic quantum numbers, i.e. quantum numbers not accessible for  $q\bar{q}$ , since this region is densely populated with ordinary  $q\bar{q}$  states. A bound system consisting of only a fermion - anti-fermion pair, i.e., a  $q\bar{q}$  system, lacks some  $J^{PC}$  states. For neutral mesons, states with  $P \neq C$  will be lacking. In contrast, a constituent boson added to a  $q\bar{q}$  pair will allow “spin-parity” exotic numbers.

Most of the searches for exotics have used hadronic production, i.e.  $\pi N$  and  $p\bar{p}(n)$  reactions characteristically yielding high statistics.  $J/\psi$  decays have been studied too, but with considerably lower statistics. So far two states have been identified as  $J^{PC} = 1^{-+}$  exotics at masses around 1.4 GeV and 1.6 GeV. It is not clear if these are hybrids or four-quark states. New experiments in different production and/or decay modes are needed.

The mass range of the observed exotic signals is accessible at current CEBAF energies. The CLAS detector is an ideal tool for studying multiparticle final states. There is already one approved experiment to search for exotic mesons in photoproduction off hydrogen.

We propose to search for an exotic state with  $I^G J^{PC} = 1^{-1^{-+}}$  in the coherent quasi-real photoproduction of  $\pi^0\eta$  and  $\pi^0\eta'$  final states on  ${}^4\text{He}$ . **Coherent production off the spin- and isospin-zero ( $S = 0$  and  $I = 0$ ) target will significantly simplify the partial-wave analysis (PWA). This is the key feature of the proposed measurements.** The measurements will be carried out using the CLAS detector in Hall B and a 6 GeV electron beam at Jefferson Lab. Experimentally, the additive quantum numbers  $C$  and  $G$  of the produced state will be determined by the identification of decay products. The final states  $\pi^0\eta$  and  $\pi^0\eta'$  will have  $G = -1$ ,  $C = +1$  and  $P = (-1)^L$ , where  $L$  is the angular momentum of produced pair. A

determination of  $J(=L)$  and, therefore,  $P$  will be done via analysis of the decay angular distribution of the final state meson, PWA.

## 2 Current status of $J^{PC} = 1^{-+}$ hybrid

### 2.1 Predictions for hybrids

The existence of a  $J^{PC} = 1^{-+}$  exotic hybrid is predicted in several different QCD models (for a review see [8, 9, 10]). All models in general predict a  $J^{PC} = 1^{-+}$  hybrid with a mass at or below 2 GeV [4, 5, 6, 11, 12]. Widths in the range  $\Gamma \sim 50 \rightarrow 200 MeV$  are favored. The decay modes are uncertain. In some models, gluonic excitation does not transfer its spin to the relative orbital angular momentum of the final state mesons', and hybrid decay to two mesons with quark S-waves does not occur. However, other models [11, 13, 14, 15] predict such a decay. It occurs through effects as spurious bag CM motion[11], or through the sequential decay of the exotic hybrid into a non-exotic hybrid and then into a conventional meson via mixing[15]. The non-exotic hybrid is mixed with a conventional meson which appears in the final state. In this description, the  $\pi\eta(\eta')$  state have small constituent gluonic components. In general  $Br_{\eta\pi} \sim 0.1$  and  $Br_{\eta\pi}/Br_{\eta'\pi} \sim 1/3$  is predicted.

### 2.2 Experimental situation

So far two states have been observed with  $J^{PC} = 1^{-+}$ ,  $\pi_1(1400)$  and  $\pi_1(1600)$ .

The  $\pi_1(1400)$  was first reported by the GAMS group[16], seen in the  $\pi^-p \rightarrow \pi^0\eta n$  channel at  $p_\pi = 100$  GeV/c. PWA of these data showed a clear  $a_2(1320) D_0$  wave, and a resonant structure in the  $P_0$ -wave at a mass of 1.4 GeV. A forward-backward asymmetry of the decay angular distribution in the Gottfried-Jackson frame of the  $\eta\pi^0$  system was observed, indicative of interfering D and P waves. It should be noted, however, that doubts have been raised about the analysis[17, 18].

The VES experiment [19] studied the reaction  $\pi^-N \rightarrow \pi^-\eta(\eta')N$  with 37 GeV beam energy. PWA analyses were done for both final states. The authors conclude that there is small resonant signal in a  $P$ -wave present around 1400 MeV.

Forward-backward decay asymmetry in the reaction  $\pi^-p \rightarrow \pi^-\eta p$  at 6.3 GeV has also been seen by the E179 collaboration at KEK[20]. PWA showed a clear  $D_+$ -wave of the  $a_2(1320)$  and a resonant structure in the  $P_+$ -wave at  $\approx 1.32$  GeV.

The Crystal Barrel collaboration studied the reactions  $\bar{p}n \rightarrow \pi^-\pi^0\eta$  and  $\bar{p}p \rightarrow \pi^0\pi^0\eta$  [21]. In order to describe the data they needed to include a  $\pi_1(1400)$  state in addition to conventional mesons.

The PWA analysis of the BNL-E852 experiment presented new evidence regarding the  $\pi_1(1400)$  [22]. They have studied reaction the  $\pi^-p \rightarrow \pi^-\eta p$  with 18 GeV beam

energy. A  $J^{PC} = 1^{-+}$  exotic wave was identified in the PWA analysis via the relative phase motion of the  $P_+$  wave with respect to the strong  $D_+$  wave of  $A_2$ .

The second  $J^{PC} = 1^{-+}$  exotic state at 1.6 GeV was observed by the VES collaboration in the final states  $\rho\pi$ ,  $\eta\pi$  and,  $\eta'\pi$  [19].

A resonance at 1.6 GeV in the  $\rho\pi$  channel was also observed in the BNL experiment. E852 carried out a PWA analysis of the  $3\pi$  system. They find a  $J^{PC} = 1^{-+}$  state at 1.6 GeV,  $\pi_1(1600)$ [23]. They also analyzed the  $\eta'\pi$  final state. A prominent resonance at 1.6 GeV was reported in this channel as well.

### 3 Proposed Experiment

The main goal of the proposed experiment is to search for a  $J^{PC} = 1^{-+}$  exotic state in the coherent production of  $\pi^0\eta$  and  $\pi^0\eta'$  final states off a  ${}^4\text{He}$  target using a 6 GeV electron beam. Photoproduction of a mesonic state in the  $t$ -channel on a spin  $S = 0$  and isospin  $I = 0$  target coherently, when target stays intact, is a powerful method to simplify significantly the PWA analysis.

The proposed reactions to study are (see Figure 1):

$$\gamma^* {}^4\text{He} \rightarrow \pi^0 \eta {}^4\text{He} \quad (1)$$

$$\gamma^* {}^4\text{He} \rightarrow \pi^0 \eta' {}^4\text{He} \quad (2)$$

Decay modes  $\pi^0 \rightarrow \gamma\gamma$  and  $\eta \rightarrow \gamma\gamma$  will be used to detect pions and etas. For the  $\eta'$  decay channels  $\eta' \rightarrow \rho^0\gamma(\pi^+\pi^-\gamma)$ , and  $\eta' \rightarrow \pi^+\pi^-\eta$  will be explored.

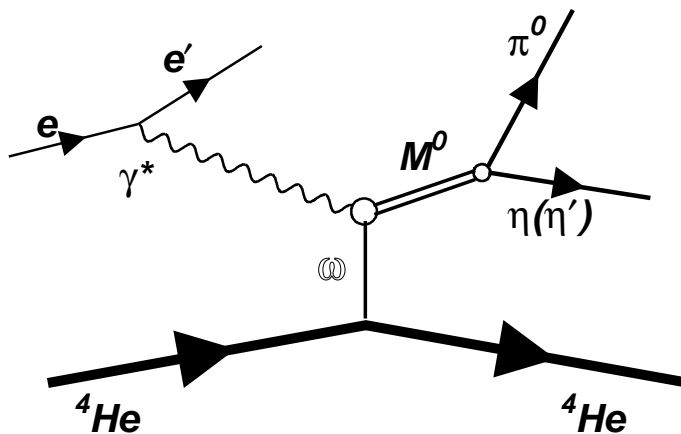


Figure 1: .

The resonance state in the  $\pi^0\eta$  and  $\pi^0\eta'$  channels will be reconstructed in the analysis of the decay angular distributions. The proposed reactions have several advantages for studying exotics:

- The final state  $\pi^0\eta$  ( $\pi^0\eta'$ ) has  $I = 1$ ,  $G = -1$ ,  $C = +1$  and  $J = (-1)^L$ , where  $L$  is the angular momentum of the final state mesons. Hence a resonance in a  $P$  wave will be an exotic  $I^G J^{PC} = 1^{-1^{-+}}$ ;
- Photo-production of the  $\pi^0\eta$  ( $\pi^0\eta'$ ) system can proceed only via  $C = -1$  exchanges. At small momentum transfer these are  $\rho^0$  or  $\omega$  exchanges, Natural Parity Exchange (NPE).
- In the coherent scattering off  ${}^4\text{He}$ , when the target nucleus stays intact, only isosinglet  $\omega$  exchange survives<sup>4</sup>.
- The helicity of the produced state will be that of the incoming photon,  $\lambda = \lambda_\gamma$ . Production of  $\pi^0\eta$  ( $\pi^0\eta'$ ) in the  $S$  state is forbidden.
- No background from  $S$ -channel baryon resonance production.

**The key feature of this experiment is that the recoiling helium nuclei stay intact. To ensure coherent production the detection of  ${}^4\text{He}$ 's in the final state is required.** This implies that due to the fast drop of the  ${}^4\text{He}$  form-factor, and due to the  $t$ -dependence of the elementary cross section, measurements should be carried out at small momentum transfer.

At small momentum transfer, close to the minimum momentum transfer required for the production of a 2 GeV mass object with 4 to 5 GeV photons, the kinetic energy of the recoiling  ${}^4\text{He}$  will be  $E_{kin} \leq 0.026$  GeV. This eliminates the possibility of using a liquid helium target since  ${}^4\text{He}$  ions at this energies will never make it out of the target. Using a gas target with the conventional photon tagging method is not an option due to the luminosity limitation caused by accidentals in the tagging system.

For these reasons we chose to use electron scattering at very small angles. This is a very attractive alternative to photoproduction. **Quasi-real photoproduction** is ideal for performing experiments on “thin” targets. The required luminosity can be achieved by increasing the primary beam intensity. The high flux of virtual photons,  $Q^2 \rightarrow 0$ , and the substantial reduction of the electromagnetic background,  $\theta > 0^\circ$ , will provide a workable “signal/accidental” ratio.

Use of the electron beam has other advantages too: a small size (few hundred  $\mu\text{m}$  diameter) high precision electron beam allows use of a small diameter target cell. That will allow to reduce the thickness of the target walls at fixed pressure (density), which is crucial for low energy recoil detection. With a small size beam the interaction point on the plane perpendicular to the direction of the beam will be better defined compared to the bremsstrahlung photon beam. This is important for defining the production vertex in multi-photon final states.

---

<sup>4</sup>In the presentation when the photon fluctuates to a vector meson and the vector meson scatters off the nucleon (VDM) the  $\omega$  exchange is the dominant one due to the larger  $\gamma\rho$  and  $\omega NN$  couplings:  $\gamma\rho = 3 \cdot \gamma\omega$ ,  $\omega NN = 4 \cdot \rho NN$ [24].

The kinematics of the proposed measurements is shown in Figs. 2 and 3. Electrons will be detected in the angular range from  $0.5^\circ$  to  $1.5^\circ$  with momenta from 0.5 to 2.5 (GeV/c). In Figure 2.a the distribution of the transfer momentum squared ( $Q^2$ ) of the electron versus the virtual photon hadron invariant mass ( $W$ ) is shown. In this energy domain the mass range in the  $t$ -channel from 1 to 2 GeV will be covered at sufficiently low momentum transferred. In Figure 2.b the momentum transferred squared in the  $t$ -channel is plotted vs the produced mass. The lower edge of the distribution corresponds to  $t_{min}$ .

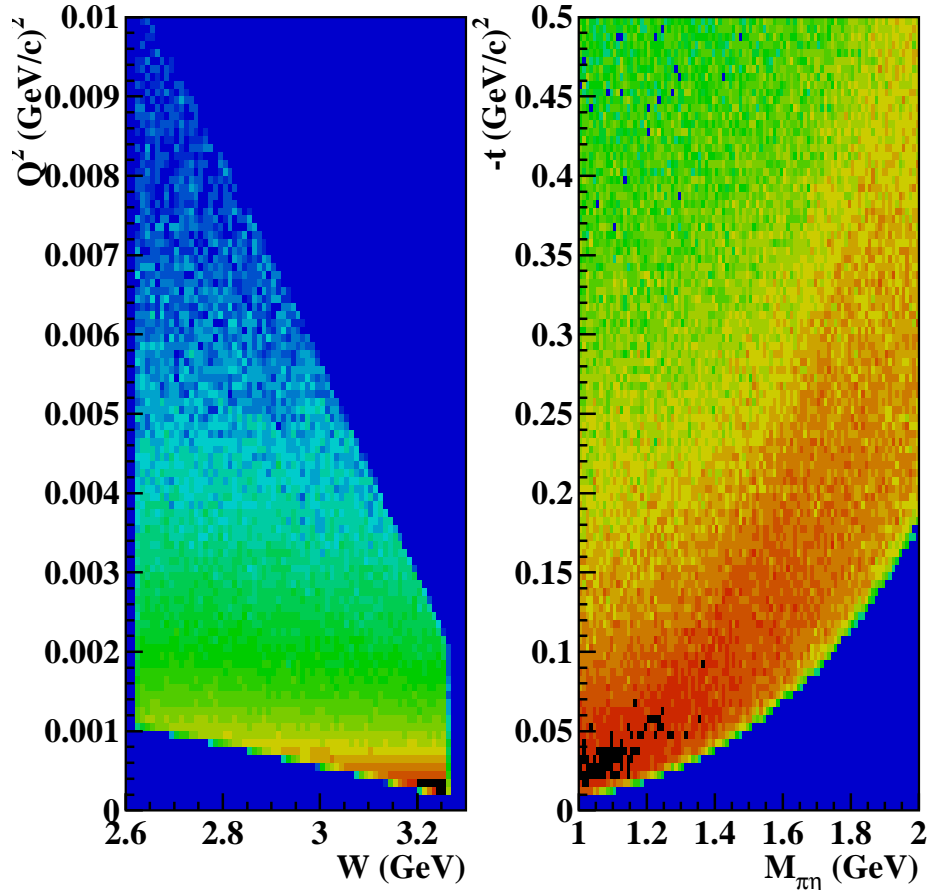


Figure 2: Kinematics of the proposed measurements. a) - electron momentum transferred squared vs the virtual photon hadron invariant mass. b) - four momentum transfer squared to the target as a function of the produced  $t$ -channel meson mass. The lower band corresponds to  $t_{min}$ .

The corresponding distribution of the kinetic energy of the recoiling  $^4\text{He}$  as a function of the mass of the produced state is shown in Figure 3.a. For the most interesting region of masses, 1.2 to 1.8 GeV, the recoiling nuclei will scatter mostly in the angular range from  $20^\circ$  to  $60^\circ$  with kinetic energies  $E_{kin} \geq 0.007$  GeV (or momentum  $p \geq 0.23$  GeV/c), Figure 3.b.

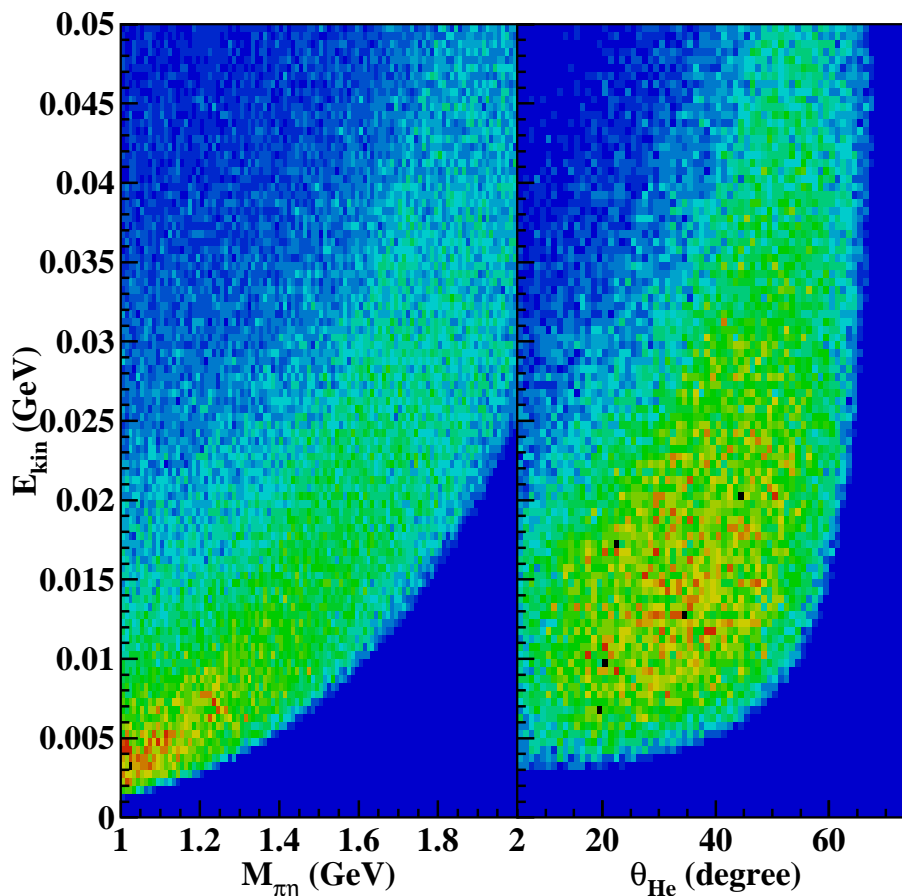


Figure 3: a) - the kinetic energy of  ${}^4\text{He}$  nuclei as a function of the mass of the produced state in the  $t$ -channel. b) - the angular and momentum distribution of recoiling nuclei for the mass range 1.2 to 1.8 GeV.

## 4 PWA Formalism.

Phase shift analysis is the key element in any meson spectroscopy experiment. The contribution of different spin and parity states decaying into the same final state particles are determined through a fit to the angular distribution of the decay products. The number of parameters in the fit, and therefore the required statistics, depends on the rank of the decay density matrix. The latter is defined by the number of spin and helicity states of incoming and outgoing particles, and on the  $t$ -channel exchange particle.

In photoproduction (as in the case of pion beams) the mechanism leading to natural parity and unnatural parity exchange (NPE and UPE) in the  $t$ -channel do not interfere, and contribute to different amplitudes with different angular dependences. In the case when the production mechanism is defined it provides additional constraints on the angular dependences of amplitude.

The differential cross section of  $\pi^0\eta$  ( $\pi^0\eta'$ ) photoproduction, in the rest frame of produced  $t$ -channel state (Gottfried-Jackson frame), can be written as<sup>5</sup>:

$$\frac{d\sigma}{d\Omega} = |A_0 + A_-|^2 + |A_+|^2, \quad (3)$$

where the helicity amplitudes of UPE are:

$$A_0 = \sum_{L=0}^{L_{max}} (2L+1)^{1/2} L_0 D_{00}^L(\Theta, \phi), \quad (4)$$

$$A_- = \sum_{L=0}^{L_{max}} \sum_{\lambda=1}^L (2L+1)^{1/2} \sqrt{2} L_{\lambda-} \text{Re}(D_{\lambda 0}^L(\Theta, \phi)), \quad (5)$$

and the amplitude for NPE is:

$$A_+ = \sum_{L=0}^{L_{max}} \sum_{\lambda=1}^L (2L+1)^{1/2} \sqrt{2} L_{\lambda+} \text{Im}(D_{\lambda 0}^L(\Theta, \phi)). \quad (6)$$

Here  $L$  is the total angular momentum of the  $\pi^0\eta$  ( $\pi^0\eta'$ ) system, and the sum goes up to the highest possible angular momentum of the produced pair in the given mass range. The second sum in Eq.(5) and Eq.(6) correspond to the possible helicity states of the pair,  $\lambda$ .  $L_0$  and  $L_{\lambda-}$  are the amplitudes for the production of  $\pi^0\eta$  ( $\pi^0\eta'$ ) with spin  $L$  via UPE,  $L_{\lambda+}$  via NPE. These amplitudes are parameters in the PWA. In each energy bin the angular distribution of the decay mesons will be analyzed to determine the production strength of a particular wave.

The function  $D_{\lambda 0}^L(\Theta, \phi)$  defines the angular distribution of  $\pi$  (or  $\eta/\eta'$ ) in the GJ frame.  $\Theta$  and  $\phi$  are the polar and azimuthal angles of the meson in that frame.

In the case of coherent photoproduction on  ${}^4\text{He}$ , when only  $\omega$  exchange is allowed (see Section 3), the amplitudes  $A_0$  and  $A_-$  will vanish, and only  $A_+$  will contribute. More, production of a state with  $L = 0$  is forbidden due to the S-channel helicity conservation (SCHC)<sup>6</sup>, and the helicity of the  $\pi^0\eta$  ( $\pi^0\eta'$ ) system should be that of the incoming photon. Thus, the expression for the differential cross section in Eq.(3) for the reaction  $\gamma {}^4\text{He} \rightarrow {}^4\text{He}\pi^0\eta$  ( $\pi^0\eta'$ ) will be reduced to:

$$\frac{d\sigma}{d\Omega} = |A_+|^2, \quad (7)$$

with

$$A_+ = \sum_{L=1}^{L_{max}} (2L+1)^{1/2} \sqrt{2} L_{1+} \text{Im}(D_{10}^L(\Theta, \phi)), \quad (8)$$

---

<sup>5</sup>Here and in the following we will use notations from Ref.[17].

<sup>6</sup>This is valid at our kinematics where  $\frac{\sqrt{-(t-t_{min})}}{E_\gamma} \sim 0$

The  $D_{10}^L(\Theta, \phi)$  function can be expressed through  $d$ -functions[30]:

$$D_{10}^L(\Theta, \phi) = d_{10}^L(\Theta) e^{i\phi}, \quad (9)$$

and the imaginary part will be:

$$\text{Im}(D_{10}^L(\Theta, \phi)) = d_{10}^L(\Theta) \sin(\phi), \quad (10)$$

One notices that the  $\sin(\phi)$  term arises from the assumption  $\lambda = \lambda_\gamma$ . This can be an independent test of the SCHC. The measured cross sections should have a  $\sin^2(\phi)$  dependence.

The coefficient functions  $d_{10}^L$  for  $P$ ,  $D$ , and  $F$  waves in final state are presented below:

$$\begin{aligned} d_{10}^1 &= -\frac{1}{\sqrt{2}} \sin(\phi), \\ d_{10}^2 &= -\sqrt{\frac{3}{2}} \sin(\phi) \cos(\Theta), \\ d_{10}^3 &= -\frac{\sqrt{3}}{4} \sin(\phi) (5 \cos^2(\Theta) - 1), \end{aligned} \quad (11)$$

Finally, the differential cross section for the production of interfering waves with  $L$  up to 3 we will be:

$$\begin{aligned} \frac{d\sigma}{d\Omega} &= | -\sqrt{3}P_{1+} \sin(\phi) \\ &+ -\sqrt{15}D_{1+} \sin(\phi) \cos(\Theta) \\ &+ -\frac{\sqrt{15}}{2}F_{1+} \sin(\phi) (5 \cos^2(\Theta) - 1) |^2, \end{aligned} \quad (12)$$

The parameters  $P_{1+}$ ,  $D_{1+}$ , and  $F_{1+}$  will be determined via the analysis of the angular distribution of the decay mesons. The exotic  $J^{PC} = 1^{-+}$  should be expected as a resonance in the energy dependence of the  $P_{1+}$ .

## 5 Experimental Issues

Final state topologies that will be analyzed for the reconstruction and identification of  $\pi^0\eta$  and  $\pi^0\eta'$  in the reactions (1) and (2) are:

- $\pi^0\eta$ 
  - $e'\gamma\gamma\gamma^4He$ : with one missing  $\gamma$ ;
  - $e'\gamma\gamma\gamma^4He$ : no missing particles;

- $\pi^0\eta' \rightarrow \pi^+\pi^-\eta; \pi^+\pi^-\gamma$ 
  - $e'\gamma\gamma\pi^+{}^4He$ : missing  $\pi^-$
  - $e'\gamma\gamma\pi^-{}^4He$ : missing  $\pi^+$
  - $e'\gamma\pi^+\pi^-{}^4He$ : missing one  $\gamma$  or two  $\gamma$ s from  $\eta$  or  $\pi^0$  decay
  - $e'\gamma\gamma\pi^+\pi^-{}^4He$ : no missing particles
  - $e'\gamma\gamma\gamma\pi^+\pi^-{}^4He$ : no missing particles

There are three main issues related to the detection of the desired final states:

1. detection and identification of the multi-particle, multi-photon final states;
2. detection of low energy ( $\geq 0.01$  GeV) recoiling  ${}^4He$  nuclei;
3. detection of the scattered electrons at small angles,  $0.5^\circ < \theta_{e'} < 1.5^\circ$ .

To carry out the proposed measurements will require some changes to the standard CLAS configuration.

## 5.1 Proposed configuration.

While CLAS in its standard configuration is doing a great job for the detection and identification of multi-particle final states, we will require to run with the configuration proposed for the DVCS experiment [25] - a solenoid shielding magnet for Møller electrons and a photon detector for small angle coverage. The solenoid field will allow to keep Møller electrons away from the recoil detector. Use of the small angle calorimeter, based on  $PbWO_4$ , will increase significantly the forward acceptance for photons. Both these devices are in the process of construction and will be ready for use in about a year.

To detect low energy recoiling  ${}^4He$  nuclei we will use the same detector that is proposed for the experiment to study neutron structure functions using low energy spectator tagging in electron deuteron scattering (the BoNuS experiment is presented to this PAC). This device will detect spectator protons in the backward direction with respect to the  $q$  vector with momenta above 60 MeV/c. A high pressure deuterium gas target combined with a Radial Time Projection Chamber (RTPC) will allow to measure a track segment, start time and energy loss of a charged particle. Gas Electron Multipliers (GEM) will be used to collect signals from the RTPC. The same device, after replacing the deuterium gas with helium, will be used in our experiment. The threshold for  ${}^4He$  detection will be 250 MeV/c. Particle identification will not be a problem since energy loss of a low energy  ${}^4He$  nucleus will be significantly higher than for pions or protons.

Finally, a new electron detector at small angles,  $0.5^\circ$  to  $1.2^\circ$ , will be required to tag electrons that interacted in the target. There are a number of experiments presently

in the development stage that will use this small angle electron detector. Some of them are presented to this PAC as letters-of-intent. Such a facility will be extremely important for conducting quasi-real photoproduction experiments at higher energies,  $E > 7$  GeV, which the present CLAS tagging system cannot reach.

Currently we have two alternative designs for the forward detector. The first is a compact device that combines a fast position detector and a high granularity crystal calorimeter. The second is a magnetic spectrometer with a momentum bite (from  $0.05E$  to  $0.45E$ ) for the angular range from  $0.5^\circ$  to  $1.2^\circ$ . The first device is in a more advanced stage of the design. All components, the fast position detector and the crystal calorimeter array have been built and used in other experiments. The down side of this device is its high rates. Which will prevent its use directly in the trigger, and will contribute to a high “accidental/signal” ratio. The design of the magnetic spectrometer is not finalized yet. The main advantage of the spectrometer is the lower singles rate. It can be used in the trigger, and will have a much improved “accidental/signal” ratio. New simulations and also beam tests, to measure the rates at small angles, will help finalize the design of the downstream detector.

## 5.2 CLAS performance.

To show how well CLAS can handle multi-particle, and particularly multi-photon, final states we analyzed data from the recent 6 GeV electron run, CLAS experiment E1-6. The goal of this analysis was to identify the reactions:

$$\begin{aligned} ep &\rightarrow (e)p\pi^0\pi^0 \\ ep &\rightarrow (e)p\pi^0\eta \end{aligned} \tag{13}$$

Similar to what we are proposing for the coherent production on  ${}^4\text{He}$ , only on the proton and without detecting the forward going electron.

The main focus of the E1-6 experiment is the measurement of electron-proton scattering in deep inelastic scattering region. Data were acquired using a “single electron” trigger. The CLAS Level 1 trigger was created by a coincidence of the forward calorimeter and the Cherenkov counter in the same sector.

Due to the “rejection” inefficiency of the Level 1 trigger, in addition to the real electron events (that account for  $< 10\%$  of the trigger rate), coincidences from “non-electron” events are recorded as well. These are hadronic events produced mostly by “0” degree scattered electrons. For the analysis of reactions in Eq.(13) we select events from “non-electron triggers” (events that did not have a reconstructed negative track) with at least one fitted positive track, and four neutral hits in the forward calorimeter:

$$ep \rightarrow p\gamma\gamma\gamma\gamma X \tag{14}$$

In Figure 4 the missing momentum vs. missing mass squared ( $M_X^2$ ) is shown for the selected sample. The  $M_X^2$  is consistent with 0 at low missing momentum. In

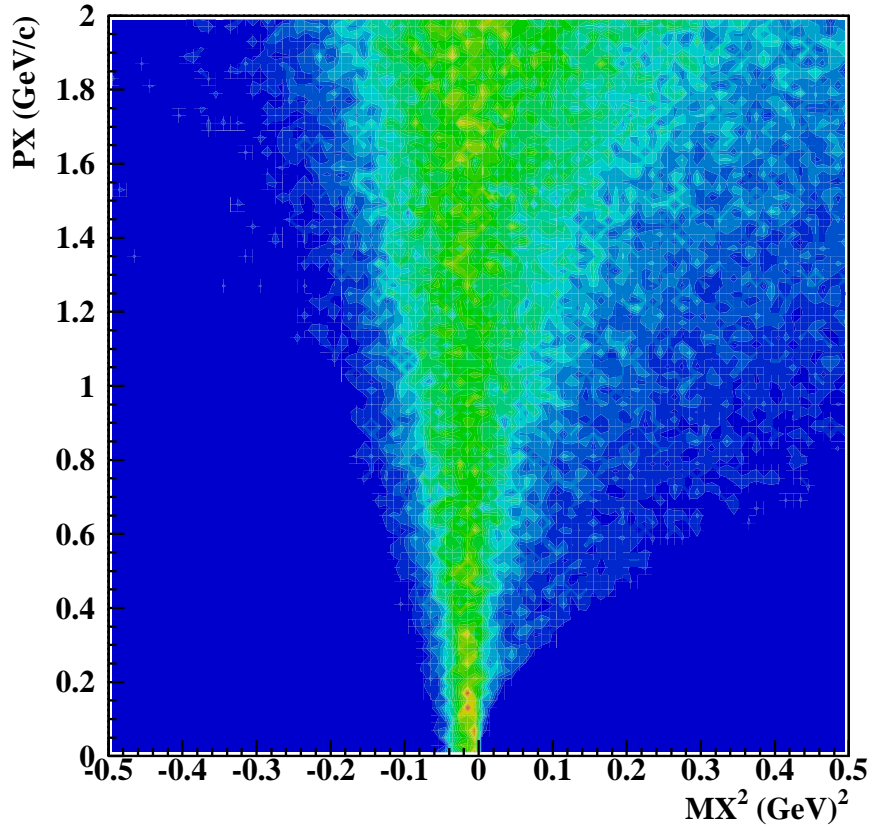
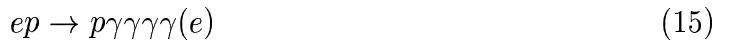


Figure 4: Distribution of the missing energy vs. missing mass squared in the reaction of Eq.(14).

addition, the distribution of the perpendicular component of the missing momentum is peaking around zero, see Figure 5. These facts suggest that the missing particle is an electron with its momentum vector pointing in the direction of the beam (electron scattered at  $\sim 0^\circ$ ). Therefore, applying cuts  $-0.1 < MM^2 < 0.1 \text{ GeV}^2$ , and  $\sqrt{(PX_x/PX)^2 + (PX_y/PX)^2} < 0.1$  we select the reaction:



(photoproduction of the  $4\gamma$  final state with a bremsstrahlung photon beam).

To select  $\pi^0\pi^0$  and  $\pi^0\eta$  final states all possible combinations of two photons have been studied. In Figure 6, the invariant mass of one pair of photons against the invariant mass of other pair is plotted. One clearly sees  $\pi^0\pi^0$  and  $\pi^0\eta$  final states. The cuts on the invariant masses of two photons used for identification of  $\pi^0$  and  $\eta$  are  $0.1 < M_{\gamma\gamma} < 0.18 \text{ GeV}$  and  $0.5 < M_{\gamma\gamma} < 0.62$ , respectively.

After identifying the reactions  $\gamma p \rightarrow p\pi^0\pi^0$  and  $\gamma p \rightarrow p\pi^0\eta$ , the invariant mass distributions for  $\pi^0\pi^0$  and  $\pi^0\eta$  are studied. The invariant mass distribution of the two  $\pi^0$ 's shown in Figure 7.a. As one expects,  $f_0(980)$  and  $f_2(1270)$  are clearly seen. The invariant mass of  $\pi^0\eta$  system is presented in Figure 7.b. There is a peak around

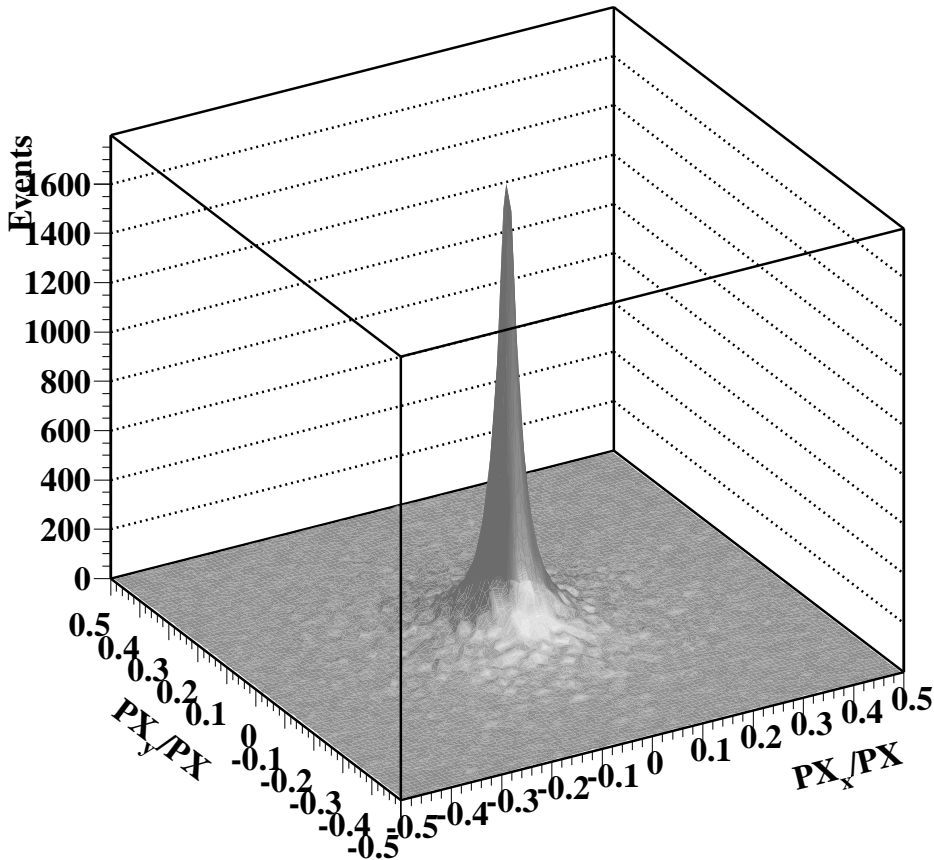


Figure 5: Component of the missing momentum perpendicular to the direction of the beam normalized to the absolute value of the missing momentum.

1 GeV where the  $a_0(980)$  is expected, and the shoulder on the falling edge around 1.3 GeV, which corresponds to the  $a_2(1320)$  meson.

These analyses, although with data taken as a byproduct and not in an efficient way, clearly show the excellent performance of the CLAS detector in the reconstruction and identification of multi-photon final states.

## 6 Cross Section and Expected Event Rate.

There is very little known about electromagnetic production cross sections for high mass meson resonances. Obviously, there are no data on the production of  $J^{PC} = 1^{-+}$  state. To estimate the cross section and the production yield for  $J^{PC} = 1^{-+}$  we use the experimentally measured  $a_2$  photoproduction cross section [26, 27] and estimates for the relative weight of  $2^{++}$  and  $1^{-+}$  waves from pion-production experiments (see discussions in Ref. [29]).

For the rate estimate we use a luminosity of  $3 \times 10^{33} \text{ cm}^{-2}\text{sec}^{-1}$ , resulting from a

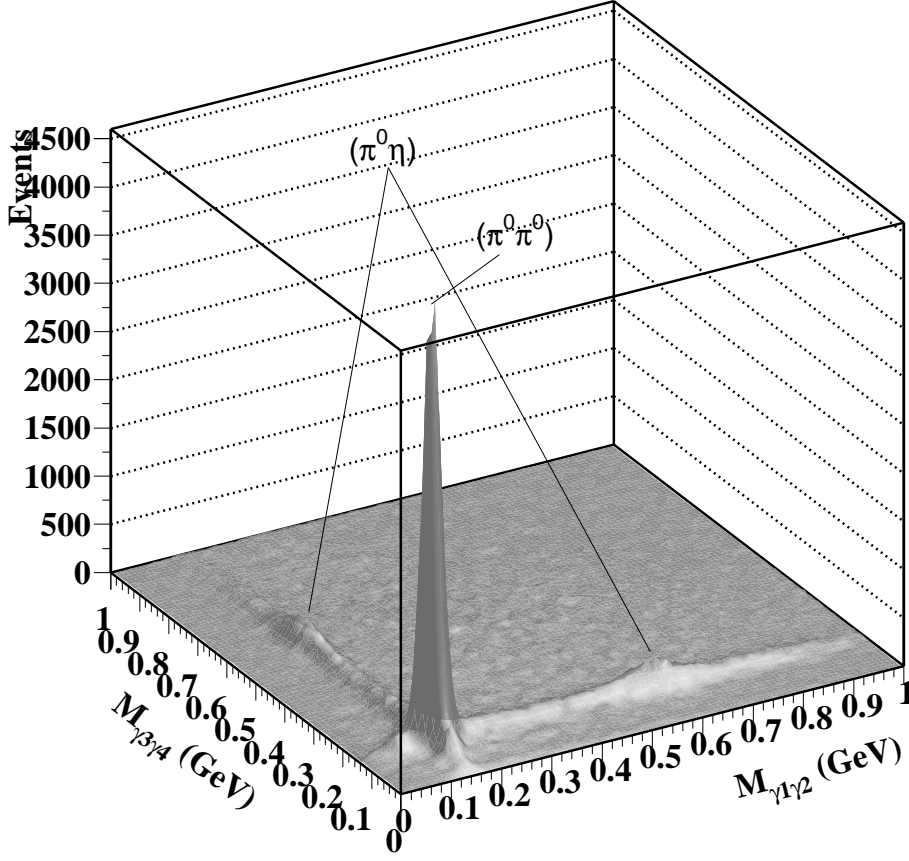


Figure 6: The invariant mass of two photons vs. the invariant mass of other two.

10 cm long 7 atm.  $^4\text{He}$  gas target and a 300 nA electron beam at 6 GeV.

## 6.1 Cross section formalism.

The cross section of  $t$ -channel meson electroproduction on a nucleon (see diagram on Figure 8), integrated over the azimuthal angle between electron and hadron planes, can be presented as a sum of cross sections for transversely ( $\sigma_T$ ), and longitudinally ( $\sigma_L$ ) polarized photons:

$$\frac{d\sigma_{eN \rightarrow eM^0N}}{dQ^2 dW dt} = \Gamma_W \cdot \left( \frac{d\sigma_T}{dt} + \epsilon \frac{d\sigma_L}{dt} \right). \quad (16)$$

Here  $\Gamma_W$  is the flux of virtual photons and is defined as:

$$\Gamma_W = \frac{\alpha}{4\pi} \cdot \frac{W^2 - m^2}{m^2 E^2} \cdot \frac{W}{Q^2} \cdot \frac{1}{1 - \epsilon}. \quad (17)$$

In the equations above,  $\epsilon$  is the virtual photon polarization and is given by:

$$\epsilon = \left( 1 + 2 \frac{Q^2 + q^{02}}{4EE' - Q^2} \right)^{-1}. \quad (18)$$

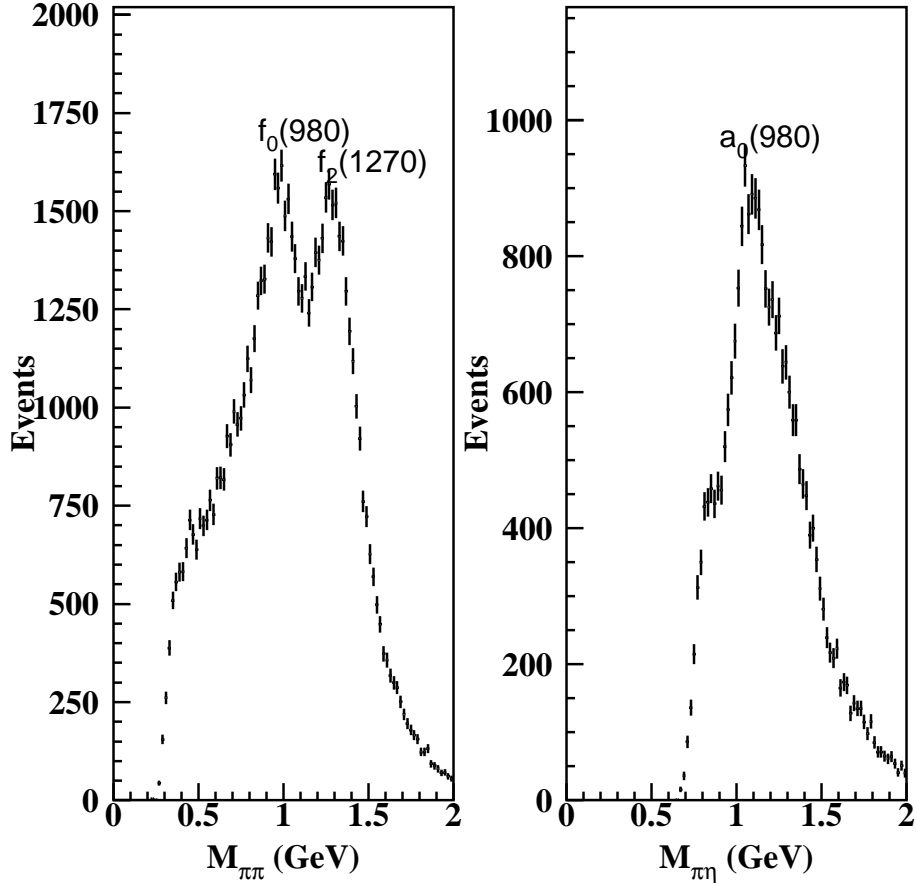


Figure 7: Invariant mass distributions for  $\pi^0\pi^0$  (left) and  $\pi^0\eta$  (right) events.

The other kinematical variables are: electron transferred momentum squared  $Q^2 = -q^{\mu 2}$  where  $q^\mu = (k^\mu - k'^\mu)$  is the four-momentum of the virtual photon, and  $k^\mu (k'^\mu)$  is the four-momentum of incoming (outgoing) electron. In Eq.(16)  $t$  is the transferred momentum squared to the target, and the mass squared of the virtual photon hadron system,  $W^2$ , is:

$$W^2 = m^2 + 2mq^0 - Q^2, \quad (19)$$

$m$  is the nucleon mass.

Using vector meson dominance (VDM) one can relate  $\sigma_T$  and  $\sigma_L$  to the photoproduction cross section [28]. The relation for  $\sigma_T$  is:

$$\sigma_T = \left( \frac{m_\rho^2}{m_\rho^2 + Q^2} \right)^2 \cdot \sigma_{\gamma N \rightarrow M^0 N}, \quad (20)$$

and for  $\sigma_L$ :

$$\sigma_L = \left( \frac{m_\rho^2}{m_\rho^2 + Q^2} \right)^2 \cdot \frac{Q^2}{m_\rho^2} \cdot (1-x)^2 \cdot \xi(Q^2, \nu) \cdot \sigma_{\gamma N \rightarrow M^0 p}, \quad (21)$$

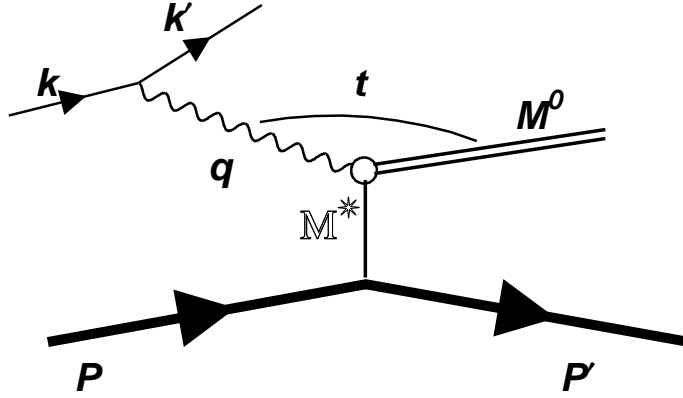


Figure 8: Diagram for electroproduction of a  $t$ -channel meson on the nucleon.

where  $m_\rho$  is the  $\rho$  meson mass, and  $\sigma_{\gamma N \rightarrow M^0 N'}$  is the photoproduction cross section.  $\xi(Q^2, \nu)$  scales the model to the data, and  $x = Q^2/(2qp)$  where  $p$  is the four-momentum of the target nucleon. One notices an extra  $Q^2$  in Eq.(21). In the kinematics of this experiment ( $Q^2 \rightarrow 0$ ) the  $\sigma_L \rightarrow 0$ , and the cross section can be approximated as:

$$\frac{d\sigma_{eN \rightarrow eM^0 N}}{dQ^2 dW dt} \simeq \Gamma_W \cdot \left( \frac{m_\rho^2}{m_\rho^2 + Q^2} \right)^2 \cdot \frac{d\sigma_{\gamma N \rightarrow M^0 N}}{dt} \simeq \Gamma_W \cdot \frac{d\sigma_{\gamma N \rightarrow M^0 N}}{dt} \quad (22)$$

Production on nuclei is usually used to enhance the statistics since in that case the resulting scattering amplitude is the sum of amplitudes for scattering from individual nucleons. In the proposed experiment the gain in the production rate (cross section) compared to the scattering off the single nucleon will be a factor of 16 (assuming that production on the proton and on the neutron are equal). However, the requirement of having a  ${}^4\text{He}$  nucleus intact will add an extra form-factor,  $F_{He}(t)$ , in the production amplitude. The cross section in Eq.(22) for the scattering on  ${}^4\text{He}$  can be expressed as:

$$\frac{d\sigma_{eHe \rightarrow eM^0 He}}{dQ^2 dW dt} = \Gamma_W \cdot \frac{d\sigma_{\gamma N \rightarrow M^0 N}}{dt} \cdot (4F_{He}(t))^2 \quad (23)$$

At the kinematics of these measurements  $\Gamma_W$  will be in the range from 0.15 to 4  $(\text{GeV}/c)^{-3}$ , see Figure 9. In Figure 10 the factor  $(A \cdot F_A(t))^2$  for  ${}^4\text{He}$  is shown as a function of the transferred momentum squared. The vertical lines in the figure correspond to  $t_{min}$  for masses 1.5 and 2 GeV at 4.5 GeV incoming photon energy. The recoil detector will allow to detect  ${}^4\text{He}$  nuclei with momenta  $p \geq 0.25$  GeV/c (or  $t \geq 0.065$   $(\text{GeV}/c)^2$ ). As one can see, the detector threshold matches well with  $t_{min}$  for the mass range of interest.

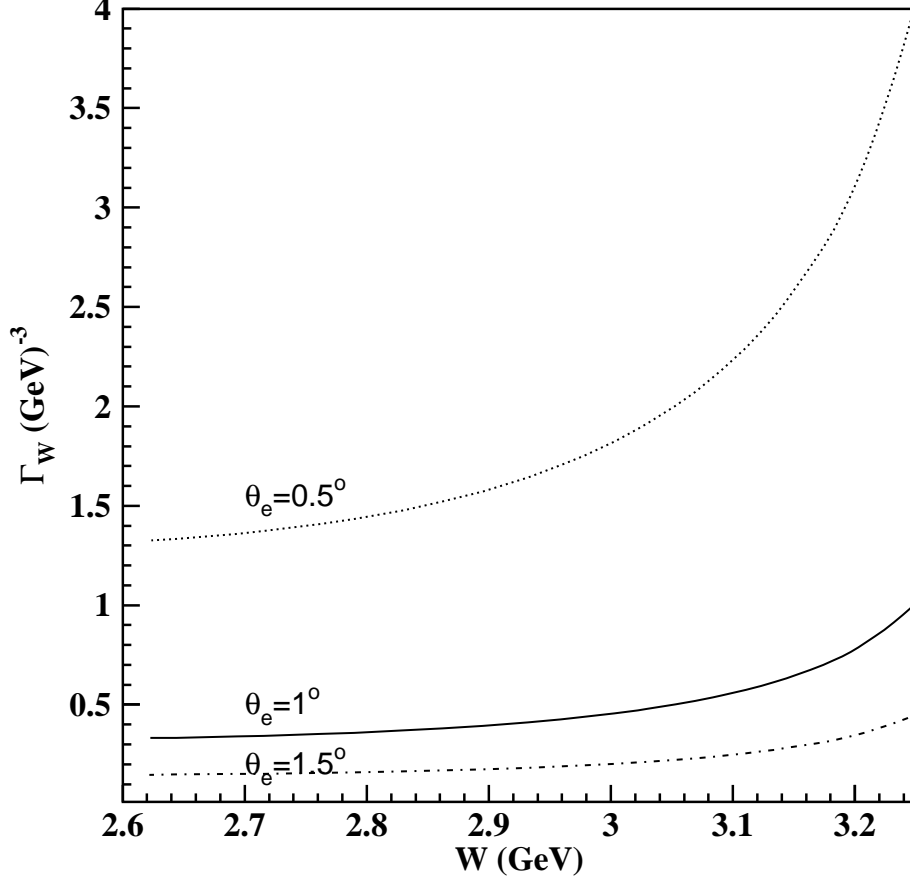


Figure 9: Dependence of  $\Gamma_W$  on  $W$  at different electron scattering angles.

## 6.2 Event rate.

To calculate the  $a_2$  electroproduction rate the photoproduction data from Ref. [26] are used. In Ref. [26] photoproduction of  $a_2$  was studied in the reaction  $\gamma p \rightarrow n\pi^+\rho^0$  at 4.3 and 5.25 GeV. We will use the 4.3 GeV data since the average photon energy in our kinematics is 4.5 GeV. The  $t_{min}$  for masses around 1.3 GeV at these energies is  $\sim 0.04$  (GeV/c)<sup>2</sup>. Since the detection threshold for recoiling  ${}^4\text{He}$  is  $p > 0.25$  GeV/c, the range of accessible  $t' = t - t_{min}$  will be  $> 0.03$ . In the range of  $t'$  from 0.03 to 0.13 (or  $t$  from 0.07 to 0.17 (GeV/c)<sup>2</sup>) the  $a_2$  photoproduction cross section, in the  $\pi\rho$  decay mode, is  $\frac{d\sigma}{dt'} = 4\mu\text{b}/(\text{GeV}/c)^2$ . Since  $a_2$  has 70% branching ratio to  $\pi\rho$  the total cross section will be  $5.7\mu\text{b}/(\text{GeV}/c)^2$ . We will study neutral channels only, and in the Ref.[26, 27] the cross section of the  $a_2^+$  was measured. The estimates for the ratio of  $a_2^0$  and  $a_2^+$  photoproduction cross sections has been done assuming  $\pi$ -exchange for the charged mode and omega exchange for the neutral. The estimated ratio is  $\frac{\sigma(\gamma p \rightarrow p A_2^0)}{\sigma(\gamma p \rightarrow p A_2^+)} \simeq 0.5$ , and therefore the estimate for the cross section for neutral  $a_2$  photoproduction is  $2.8\mu\text{b}/(\text{GeV}/c)^2$ .

Inserting this result into Eq.(23), and taking a factor  $(A \cdot F_A(t))^2 = 2$  for  $t = 0.12$

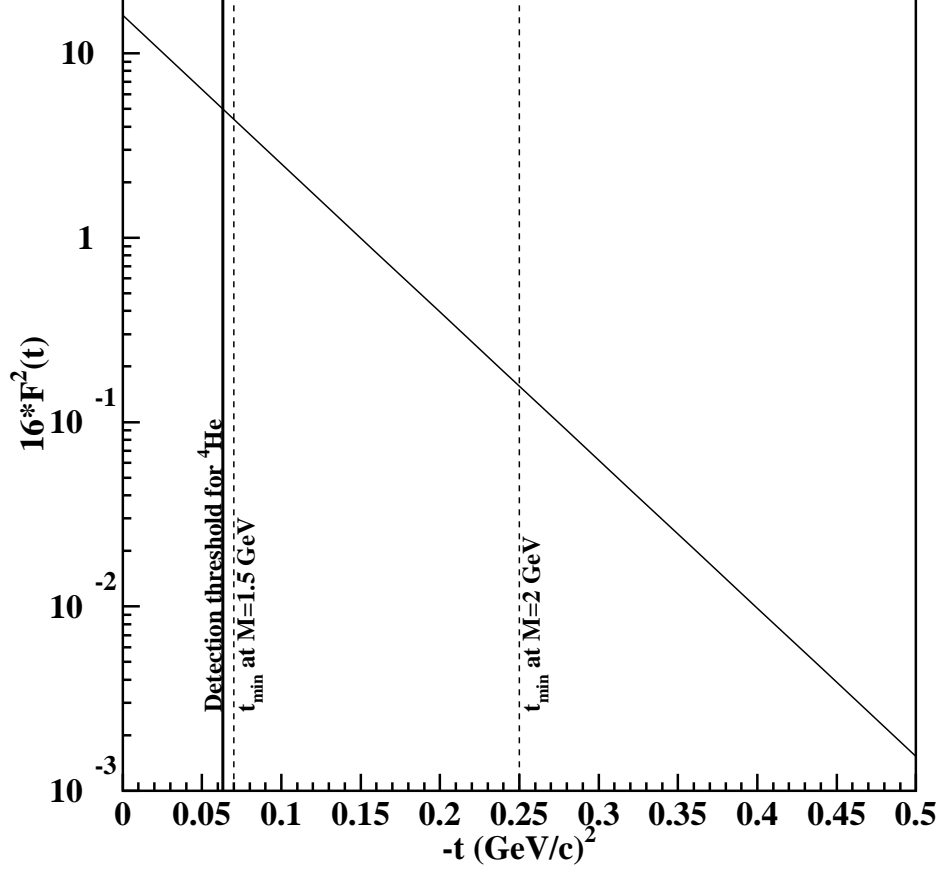


Figure 10: Factor  $(A \cdot F_A(t))^2$  for  ${}^4\text{He}$  as a function of transferred momentum squared  $t$ . The vertical solid line corresponds to the detection threshold of  ${}^4\text{He}$ . The vertical dashed lines correspond to  $t_{\min}$  for the production of final states with 1.5 and 2 GeV masses, accordingly, at 4.5 GeV incoming photon energy.

$(\text{GeV}/c)^2$ , and the average  $\Gamma_W = 0.7 (\text{GeV}/c)^{-3}$  we find the differential cross section of the  $a_2^0$  electroproduction w  $\frac{d\sigma_{eHe \rightarrow eM^0He}}{dQ^2 dW dt'} = 3.98 \mu b (\text{GeV}/c)^{-5}$ .

The following parameters have been used to estimate the  $A_2$  detection rate in the  $\pi^0\eta \rightarrow \gamma\gamma\gamma\gamma$  channel:  $\Delta W = 0.6 \text{ GeV}$ ;  $\Delta Q^2 = 0.008 (\text{GeV}/c)^2$ ,  $\Delta t' = 0.1 (\text{GeV}/c)^2$ ,  $L = 3 \times 10^{33} \text{ cm}^{-2} \text{ sec}^{-1}$ , acceptance  $A \simeq 0.05$ , and the  $\text{Br}(A_2 \rightarrow \pi^0\eta) \times \text{Br}(\eta \rightarrow \gamma\gamma) = 0.14 \times 0.39 = 0.0546$ [30]. This yields a detection rate for  $a_2^0$  in the  $(\gamma\gamma\gamma\gamma)$  final state  $N_{A_2} \simeq 56 \text{ hour}^{-1}$ .

As mentioned above one might expect a  $1 : 10$  ratio for the  $1^{-+} : 2^{++}$  production rate in the  $\pi^0\eta$  channel, [29]. Using the expected rate of  $a_2^0$  we found that the expected rate for an exotic wave will be  $\sim 5.6 \text{ hour}^{-1}$ . For 720 hours of running with a luminosity of  $L = 3 \times 10^{33} \text{ cm}^{-2} \text{ sec}^{-1}$ , we expect to detect in the  $4\gamma$  final state 4000  $\pi^0\eta$  with  $J^{PC} = 1^{-+}$  exotic quantum numbers. There will be about 40000  $a_2^0$ 's detected in the  $4\gamma$  decay mode. Within a month of running we will be able to collect more data in the  $\pi^0\eta$  channel than any previous experiment. For comparison in the

E852 [22] the total number of  $\pi^-\eta$  events in the mass range  $0.8 < M(\pi\eta) < 1.85$  GeV was about 38000, in our experiment we expect 44000  $4\gamma$  decays to be detected from  $a_2^0$  and exotic mesons only

## 7 Other Possible Channels

Although the main focus of the proposed measurements are reactions presented in Eq.(1) and Eq.(2), due to the open acceptance of CLAS many other final states will be recorded in parallel. For the reasons stated above the coherent production on  $^4\text{He}$  will put constraints on the production mechanism of different final states and will simplify the PWA analysis. This will allow to extend the studies of exotic states to other decay modes.

### 7.1 Search for exotic meson in the $\phi\pi$ final state.

One very attractive method to identify exotic mesons is through the  $\phi\pi$  decay mode. Any  $s\bar{s}$ -meson decay to  $\phi\pi$  is forbidden due to the conservation of isotopic spin. This decay mode is forbidden by the Okubo-Zweig-Iizuka (OZI) rule for any  $n\bar{n}$ -meson (where  $n$  is  $u$  or  $d$  quarks) as well. On the other side, multi-quark or hybrid mesons may have a strong coupling to the  $\phi\pi$  system. The discovery of a  $\phi\pi$  resonance would indicate a new kind of hadron and suggest a  $q\bar{q}g$  or  $q\bar{q}q\bar{q}$  state. This is true for  $f'\pi$  and  $\psi\pi$  decay modes as well[31].

There is some experimental evidence for the existence of a resonance with strong  $\phi\pi$  coupling. In experiments at the LEPTON-F spectrometer[32, 33] the charge exchange reaction

$$\pi^- p \rightarrow (\phi\pi^0)n, \quad (24)$$

has been studied at a  $\pi^-$ -momentum of 32 GeV/c. In the mass spectrum of the  $\phi\pi^0$  system a new meson, C(1480), with mass  $1480 \pm 40$  MeV and width  $130 \pm 60$  MeV, was observed. The angular distributions of the sequential decay  $C(1480) \rightarrow \phi\pi^0, \phi \rightarrow K^+K^-$  have been studied, and the quantum numbers for C(1480) meson have been determined:  $I^G = 1^+, J^{PC} = 1^{--}$ . For this meson an anomalously large value of the ratio

$$BR(C(1480) \rightarrow \phi\pi^0)/BR(C(1480) \rightarrow \omega\pi^0) > 0.5 \quad (25)$$

at 95% C.L. has been obtained. This value is more than two orders of magnitude higher than the expected ratio for mesons with the standard isovector quark structure. At the present time the only consistent explanation of these properties can be obtained with the assumption that the C(1480) meson is a four quark or hybrid state.

At the  $\Omega$ -spectrometer[34] the cross section for the reaction  $\gamma p \rightarrow \phi\pi^0 p$  has been measured. Although the number of events is not large ( $\sim 25$ ), an excess of events in

the mass spectrum of the  $\phi\pi^0$  system at  $\sim 1.4$  GeV is observed. The  $\phi\pi^0$  photoproduction cross section was estimated as

$$\sigma(\gamma p \rightarrow \phi\pi^0 p) = 6 \pm 3\text{nb} \quad (26)$$

(at 95% C.L.)

The existence of the structure in the same mass range was confirmed with the study of inclusive  $\phi\pi^+$  production with a pion beam[35].

Photoproduction (or low  $Q^2$  electroproduction) is likely to be one of the more promising mechanisms for the production of exotic mesons with hidden strangeness due to the relatively large  $s\bar{s}$  content of the photon. Photons are also expected to be efficient in the production of spin-1 hybrids.

The CLAS spectrometer has excellent momentum and angular resolution and particle identification. The first attempts to explore existing CLAS data from runs g6a and g6b showed that the multiparticle reactions

$$\gamma p \rightarrow (\phi\pi^0)p, \quad \phi \rightarrow K^+K^-, \quad \pi^0 \rightarrow \gamma\gamma \quad (27)$$

$$\gamma p \rightarrow (\phi\pi^+)n, \quad \phi \rightarrow K^+K^- \quad (28)$$

can be investigated successfully [36]. In the production on a nucleon the main background to the mesonic state that decays to  $\phi\pi$  is coming from the excitation of the baryon resonances, e.g.

$$\gamma^* p \rightarrow \phi\Delta, \quad \Delta \rightarrow p\pi^0 \quad (29)$$

Coherent production of  $\phi\pi^0$  on  ${}^4\text{He}$  is a powerful tool to suppress background from any isobar excitations, and a resonance produced in the reaction:

$$\gamma^* {}^4\text{He} \rightarrow \phi\pi^0 {}^4\text{He}, \quad \phi \rightarrow K^+K^-, \quad \pi^0 \rightarrow \gamma\gamma \quad (30)$$

will be an exotic state.

## 8 Summary

QCD based models allow the existence of hybrids, hadrons having a constituent gluon in addition to the constituent quarks. Hybrid mesons can have exotic  $J^{PC}$  or  $J^{PG}$  quantum numbers, different from those of a  $q\bar{q}$  pair. Mesons with exotic quantum numbers offer a unique signature for hybrids.

This experiment will search for a  $J^{PC} = 1^{-+}$ ,  $J^{PG} = 1^{--}$  exotic signal in the coherent electroproduction off  ${}^4\text{He}$  using the Hall B CLAS detector. The mass range of  $\pi^0\eta$  and  $\pi^0\eta'$  up to  $\approx 2$  GeV will be explored. The  $J^{PC} = 1^{-+}$  exotic will be unambiguously reconstructed through the analysis of the decay angular distributions of the final state mesons. The zero spin and isospin of the target will dramatically

simplify the Partial Wave Analysis. There will be no background from  $S$ -channel nucleon resonances.

In 30 days of running with a 10 cm long, 7 atm. helium gas target with a 6 GeV electron beam at 300 nA current we will collect 40000  $a_2^0 \rightarrow \pi^0\eta$  events and about 4000 events from exotic  $J^{PC} = 1^{-+}$ state.

## References

- [1] D.Horn and J.Mandula, *Phys. Rev. D*17, 1978, p898
- [2] T. H. Burnett and Stephen R. Sharpe, Annual Reviews of Nuclear Science, Vol. 40, p. 327
- [3] L. G. Landsberg, Physics of Atomic Nuclei, Vol. 57, p. 42 (1994)
- [4] N. Isgur, R. Kokoski and J. Paton, *Phys. Rev. Lett.* 54, 1985, p.869.
- [5] F. deViron and J. Weyers *Nucl. Phys. B*185, 1981, p.391.
- [6] I.I. Balitsky, D.I. Dyakonov and A.V. Yung, *Z Phys. C*33, 1986, p.265.
- [7] Zhenping Li, Hadrons '91, S. Oneda and D. C. Peaslee, Eds., World Scientific, 1992, p. 726
- [8] T. Barnes, hep-ph/0007296.
- [9] *Proc. of the 2nd Int. Conf. on Hadron Spectroscopy*, 1987, Tsukuba, Japan.  
*Glueballs, Hybrids and Exotic Hadrons: Workshop*, 1988, Upton, NY.  
*Hadron-89: Proc. of the 3rd Int. Conf. on Hadron Spectroscopy*, 1989, Ajaccio, Corsica.  
*Hadron-91: Proc. of the 4th Int. Conf. on Hadron Spectroscopy*, 1991, College Park, Maryland.
- [10] L. Landsberg, *Preprint of IHEP 91-180, Parts I and II* 1991, Protvino.  
S.-U. Chung, *Nucl. Phys. A*473, 1988, p.511; *Z Phys. C*46, 1990, p.111.
- [11] M. Chanowitz and S. Sharpe, *Nucl. Phys. B*222, 1983, p.211.
- [12] T. Barnes, F.E. Close and F. deViron, *Nucl. Phys. B*224 1983, p.241.
- [13] F. Close and H. Lipkin *Phys. Lett. B*196, 1987, p.245.
- [14] S.Taun et al. *Phys. Lett. B*213, 1988, p.537
- [15] M.Tanimoto *Phys. Rev D*27, 2648 (1983).
- [16] D. Alde et al., *Phys. Lett. B*205, 397 (1988).
- [17] I.G. Aznauryan, *Z.Phys. C* 68, 459 (1995).
- [18] Y.D. Prokoshkin and S.A. Sadovskii, Physics of Atomic Nuclei **58**, 606 (1995).
- [19] G.M. Beladidze et al., *Phys. Lett. B*313, 276 (1993).

- [20] H. Aoyagi et al., *Phys. Lett. B* **314**, 246 (1993).
- [21] A. Abele et al., *Phys. Lett. B* **423**, 175 (1998); *Phys. Lett. B* **446**, 349 (1998).
- [22] S.U. Chung et al., *Phys. Rev. D* **60**, 092001-1 (2001).
- [23] G.S. Adams et al., *Phys. Rev. Lett.* **81**, 5760 (1998).
- [24] O.Dumbrajs et al., *Nucl. Phys. B* **216**, 1983, p277
- [25] V. Burkert, L. Elouadrhiri, M. Garçon, S. Stepanyan, CLAS experiment E-01-113.
- [26] Y. Eisenberg et al., *Phys. Rev. Lett.* **23**, 1322 (1972).
- [27] Y. Eisenberg et al., *Phys. Rev. D* **5**, 15 (1972).
- [28] J. Sakurai, *Phys. Rev. Lett.* **22**, 981 (1969).
- [29] A. Szczepaniak and M. Swat, *hep-ph/0105329* (2001).
- [30] Particle Data Group, *Phys. Rev. D* **66** (2002).
- [31] F.E. Close and H.J. Lipkin, *Phys. Rev. Lett.* **41**, 1263 (1978).
- [32] S.I. Bitjukov et al., *Sov.J.Nucl.Phys.* **38**, 1205 (1983).
- [33] S.I. Bitjukov et al., *Phys. Lett.* **B188**, 383 (1987).
- [34] M. Atkinson et al., *Nucl. Phys.* **B231**, 1 (1984).
- [35] Yu.M. Antipov et al., *Pis'ma JETP* **38**, 356 (1983).
- [36] Valery Kubarovsky,  $\phi\pi$  Photoproduction and Search for Exotic Meson with CLAS, CLAS-ANALYSIS Note 2000-001.